Available online at www.sciencedirect.com
SCIENCE DIRECT®
Journal of Power Sources 130 (2004) 221–226
JOURNAL OF POWER SOURCES
www.elsevier.com/locate/jpowsour

In situ neutron radiography of lithium-ion batteries: the gas evolution on graphite electrodes during the charging

D. Goers, M. Holzapfel, W. Scheifele, E. Lehmann, P. Vontobel, P. Novák*

Paul Scherrer Institut, CH-5232 Villigen PSI, Switzerland

Received 21 July 2003; received in revised form 17 November 2003; accepted 24 November 2003

Abstract

In situ neutron radiography (NR) was used to study the gas evolution on graphite electrodes in lithium-ion cells containing different PVDF-based gel-type electrolytes. The amount of gas bubbles and channels was calculated by image analysis. Gas production was extremely high in the case of the electrolyte containing ethylene carbonate (EC) and propylene carbonate (PC) (2:3, w/w), 1 M $LiClO_4$. About 60% of the electrode surface consisted of the gas phase which resulted in an inhomogeneous local current distribution. In contrast, the electrolyte containing EC and γ-butyrolactone (GBL) (1:1, w/w), 1 M $LiBF_4$ only showed a small increase of the gas volume between the electrodes of about 3%. In situ NR also revealed the displacement of the electrolyte due to gas evolution and volume changes of the electrodes.

Keywords: Neutron radiography; Lithium-ion batteries; Graphite electrodes

1. Introduction

In situ techniques are useful to study the charge/discharge processes occurring in lithium-ion batteries [1–3]. The formation of gas during the first charge of these batteries is an important criterion for the choice of electrode materials and the electrolyte solution. High amounts of gas evolved would cause severe leakage and safety problems. We reported that the kind of the evolved gases can be determined using differential electrochemical mass spectrometry (DEMS) [4–6]. However, using DEMS it is difficult to determine the total gas volume. Furthermore, the interest in both, the spatial distribution and kinetic behavior of the gas evolution as well as the sensitivity of a lithium-ion battery towards humidity necessitate a rapid and non-destructive inspection method to observe the battery during electrochemical cycling.

Neutron radiography (NR) has been developed to study various technical devices and archaeological objects [7,8]. The application of NR to lithium-ion batteries is very interesting due to the favorable properties with respect to mass attenuation on materials commonly used in these batteries, above all the strong attenuation by hydrogen-containing materials. We applied this technique to commercial lithium-ion batteries in order to study both, the production of gas and the level of the electrolyte solution, under practical conditions [9]. However, the use of arbitrary combinations of electrode materials and electrolytes, in particular those producing a larger gas volume, requires specially designed laboratory test cells.

We developed such a cell, which allows the study of both, the gas evolution rate and the gas spatial distribution. The goal was to compare different electrolyte solutions and to show the consequences of their choice for the electrochemical behavior of the lithium-ion cell. Two extreme cases were chosen for demonstration in this publication: (i) a propylene carbonate (PC) based electrolyte known to cause important graphite exfoliation under production of propylene gas, and (ii) an ethylene carbonate (EC)/γ-butyrolactone (GBL) based electrolyte which shows only minor emission of gas [5,10–12].

2. Experimental

2.1. Lithium-ion cells and electrochemical cycling

A specially designed laboratory test cell was developed. The schematic drawing of the cell is shown in Fig. 1. Both, the cell housing and the current collector plates were made of aluminum, known to have only a small cross section for the neutron beam [9]. To avoid alloying of lithium with the aluminum current collector plate of the negative electrode,

* Corresponding author. Tel.: +41-56-310-2457; fax: +41-56-310-4415.
E-mail address: petr.novak@psi.ch (P. Novák).

0378-7753/$ – see front matter © 2004 Elsevier B.V. All rights reserved.
doi:10.1016/j.jpowsour.2003.11.065

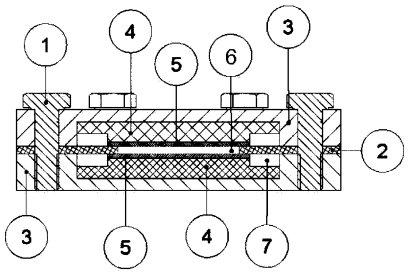

Fig. 1. Schematic representation of the NR cell. (1) Polyamide bolts, (2) polypropylene sealing ring, (3) aluminum cell housing, (4) current collector plates, (5) electrodes, (6) gel-type electrolyte, (7) gas space.

the aluminum was electroplated with copper (20 μm). The negative electrodes were made of 90% TIMREX® SLP30 graphite (TIMCAL SA) and 10% PVDF binder (SOLEF® 1015) in the case of the PC-based electrolyte. For the GBL-based electrolytes, 90% TIMREX® SFG15 (TIMCAL SA) and 10% PVDF binder (SOLEF® 1015, Solvay SA) were chosen. The electrode materials were coated on a current collector foil (copper, 20 μm). To avoid radioactive activation, a non-cobalt-based positive electrode material was chosen, $LiMn_2O_4$ spinel (Honeywell, type 13072) on a 20 μm aluminum foil. The spinel does not show noticeable gas evolution when moderately charged. The positive electrodes were composed of 85.7% active mass, 4.75% Oppanol binder (B200, BASF AG), and 9.55% mixture of carbon black (Ensaco® 250, 15%) and graphite (TIMREX® MB15, 85%). The electrodes were prepared by doctor-blading a slurry containing the electrode material and additional solvents (*N*-methylpyrrolidone for graphite electrodes and petrol ether for the spinel electrodes) onto the copper or aluminum foil, respectively.

The electrolytes used were EC:PC (2:3, w/w), 1 M $LiClO_4$ and EC:GBL (1:1, w/w), 1 M $LiBF_4$, respectively. The electrolyte components were used as received from Merck KGaA (Darmstadt, Germany). The gel was prepared by dissolving 4% PVDF (Kynar Flex® 2801) in the respective electrolyte solutions under heating.

The cell was assembled in a high-purity-argon-filled glove box to avoid any interaction with water and oxygen, both detrimental to the proper functioning of a lithium-ion battery. Moreover, if reduced, trace water would give rise to additional gas production by the formation of hydrogen. No separator was used in order to reduce the neutron absorption and allow for better visibility of gas bubbles in the cell. A constant distance between the electrodes was ensured by a 1 mm thick polypropylene ring, which acted as a sealing ring for the cell at the same time (see Figs. 1 and 2). A gel-type electrolyte was used to immobilize the evolved gas bubbles and thus, facilitate their observation. The hot electrolyte was poured onto the graphite electrode and then the cell was rapidly assembled. The gel formed upon the subsequent cooling of the electrolyte.

The amounts of active electrode masses were balanced to assure an excess of the positive spinel material, thus keeping the charge state of the spinel low and render the cell graphite-limited. An overview of the materials used in the cells discussed here is given in Table 1.

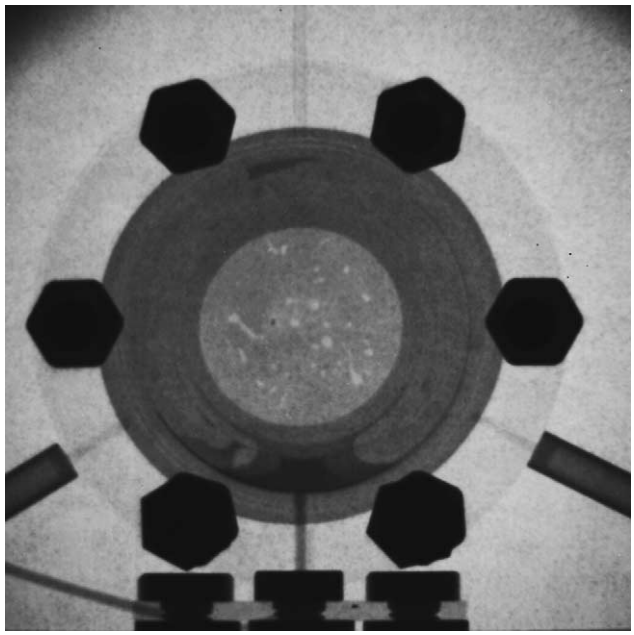

Fig. 2. NR image of the cell A prior to the electrochemical investigation.

Electrochemical experiments were carried out using a computer-controlled cell capture system (CCCC, Astrol Electronics AG, Switzerland). The current rate was set to C/4 with respect to the graphite electrode. The cut-off voltage during the charging was 4.3 V (CC mode, constant current). The cell was further kept at this voltage and the current allowed to decrease (CV mode, constant voltage).

2.2. Neutron radiography

The NR images were recorded at position 2 of the thermal neutron radiography facility NEUTRA (http://neutra.web.psi.ch/facility/index.html) of the spallation neutron source SINQ at the Paul Scherrer Institute [13]. The cell was mounted perpendicularly with respect to the neutron beam with an intensity of 5×10^6 n/(cm^2 s). Images were recorded every 2 min during electrochemical cycling. The exposure time per image was set to 20 s. The neutrons were partially absorbed depending on the local neutron transmission characteristics of the cell at each position and collected on a 0.25 mm thick neutron-sensitive scintillation screen (zinc sulfide doped with ^{6}Li). The scintillation light

Table 1
Cells investigated with in situ NR

Cell	Graphite	Electrolyte	Oxide
A	SLP30	EC:PC = 2:3, 1 M $LiClO_4$	$LiMn_2O_4$[a]
B	SFG15	EC:GBL = 1:1, 1 M $LiBF_4$	$LiMn_2O_4$[a]

[a] Honeywell AG (Seelze, Germany), type 13072.

was recorded using a Peltier-cooled CCD camera with a 1024 × 1024 pixel chip DV 434 from Andor Technology (http://www.andor-tech.com). The lateral resolution is ca. 140 μm depending on the camera objective used. The NR images were normalized using intensity information of the upper left edge region of each image, which is not expected to reveal any changes during the investigation. This procedure takes into account the different intensities of the neutron beam at each time. For illustration, differential images were calculated by the ratio of the image at the desired time and the reference image recorded before switching the current on.

3. Results and discussion

Fig. 2 shows the NR image of the in situ cell. The area of interest, representing the properties of the two electrodes and the gel-type electrolyte, can be found as the lighter circle in the middle of the image. Gas bubbles coming from the argon imprisoned in the electrolyte upon the cell assembly are seen as inhomogeneities and do not disturb the measurement. The varying intensity outside of the central circle is due to the gel electrolyte that flew besides the electrode area upon the cell assembly. It can be assumed that this does not affect the electrochemical behavior of the cell. In the outer part of the image, the polyamide bolts can be seen in dark due to the high neutron attenuation of the polymer. The two cannulae, which can be used for an optional filling-in of a liquid electrolyte, as well as the cable connectors, are also visible in Fig. 2.

3.1. PC-based electrolyte

The first half cycle (charge step) of the lithium-ion cell assembled with the PC-containing electrolyte is shown in Fig. 3. Due to the limited beam time at the neutron source, image recording was stopped at the marked position. The electrochemical behavior of this cell is poor due to the known

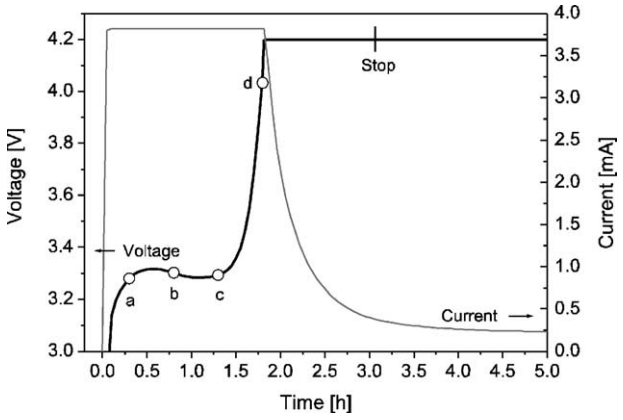

Fig. 3. Part of the first half cycle of the cell A. The NR image recording was stopped at the indicated position. The letters indicate selected images of this series shown in Fig. 4a-d.

graphite exfoliation process; the PC (and EC) reduces under gas evolution at a synthetic graphite negative electrode [10–12]. The extended voltage plateau at about 3.3 V corresponds to a significant irreversible charge consumption, and a large amount of gas is evolved. Our DEMS studies have shown that the gas emission can be correlated with this voltage plateau [4]. The gas consists mostly of propylene, which is formed during the reduction processes of PC on the negative electrode surface. According to the DEMS results, the gas evolution starts immediately after this voltage plateau is reached. The gas is visible as small bubbles (light positions) in the outer zone of the electrode area (Fig. 4b).

During the charge of the lithium-ion cell, the production of gas seems to increase and various channels, especially towards the top of the cell, are formed. At the same time, the electrolyte level rises in the zone around the electrodes. Post mortem analysis of the cell revealed that the gel electrolyte undergoes a phase separation. The polymer component remains between the electrodes and forms the walls of the channels. The liquid components were pressed out and increased the electrolyte level visible in the area around the electrodes. We observed that the yellow, fully charged compound LiC_6 was present only at the positions where no gas emission was detected during the in situ NR experiments. This fact underlines the necessity to avoid extensive gas evolution in lithium-ion batteries, since the local current density distribution becomes very heterogeneous and the practical specific charge, i.e. the charge capacity of the battery, is significantly reduced. In the case of the PC-containing electrolyte, the extent of formed gas channels is extremely high (Fig. 4d), leading to the displacement of more than 60% of the electrolyte.

A graph showing the gas amount between the electrodes as a function of the charge state is given in Fig. 5. The percentage of the electrode area covered by gas is calculated based on the NR images, taking into account the average intensity of the space filled with the electrolyte and the average intensity of the gas bubbles. Based on pixel intensity analysis, the percentage of lighter pixels within the area of interest represents the gas bubbles or channels, respectively. Due to the high amount of gas evolved in this cell, the absolute gas volume cannot be estimated because the gas left the central area to some extent and may also be dissolved in the electrolyte. However, the percentage of gas bubbles and/or channels helps to characterize the amount of gas evolved.

3.2. GBL-based electrolyte

The use of EC:GBL mixtures is favorable for gel type electrolytes and requires the presence of $LiBF_4$ to obtain satisfactory electrochemical cycling results with graphite negative electrodes [14]. It is also reported in the literature that, GBL-based electrolytes could reduce the amount of evolved gases during the formation of the solid electrolyte interphase (SEI) in the first charge step compared with EC:DMC (dimethyl carbonate) electrolyte solutions

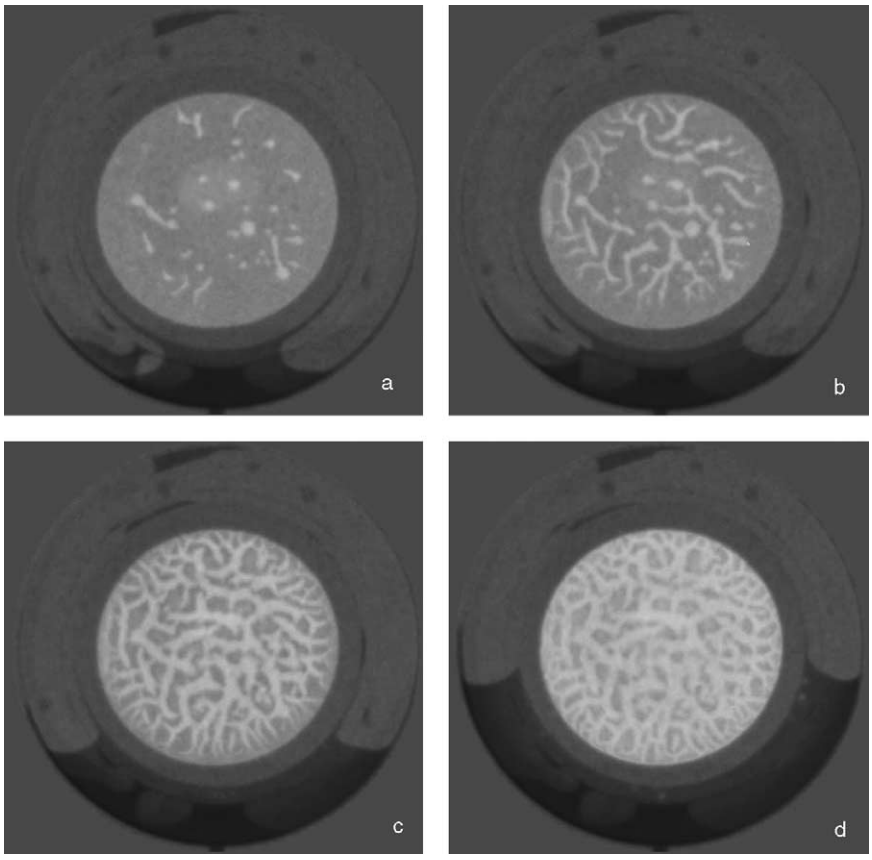

Fig. 4. (a–d) Selected normalized NR images of cell A. The correlation with the electrochemical data is indicated in Fig. 3.

[5]. This motivated us to investigate a lithium-ion cell with a GBL-containing electrolyte using NR.

Fig. 6 shows the electrochemical behavior of the GBL-containing cell in the first cycle. In contrast to the PC-containing electrolyte described in the chapter above, the irreversible charge loss is much lower (ca. 20%; the reversible capacity being approximately 350 Ah/kg with respect to the graphite). There is no indication of an enlarged voltage plateau due to extensive electrolyte decomposition. However, the special design of the NR cell causes a large IR-drop due to the relatively large distance between the electrodes. The charge behavior shows that the constant current charge phase is very short followed by a long constant voltage phase. DEMS investigations of this electrolyte suggest the formation of hydrogen during the formation of the SEI [5]. However, the amount of the gas seems to be

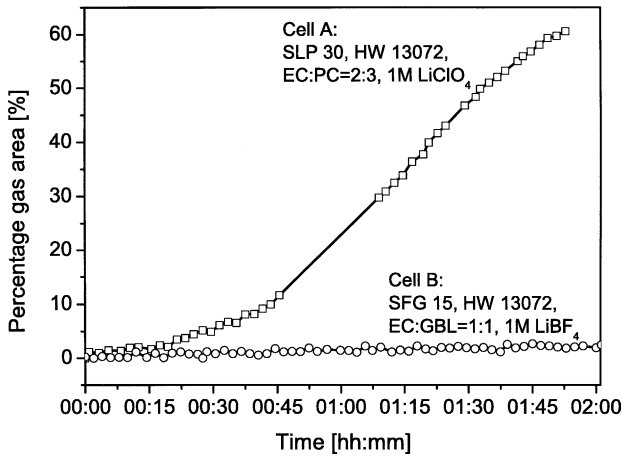

Fig. 5. Evolution of the percentage of the electrode area covered with gas bubbles, for cells A and B.

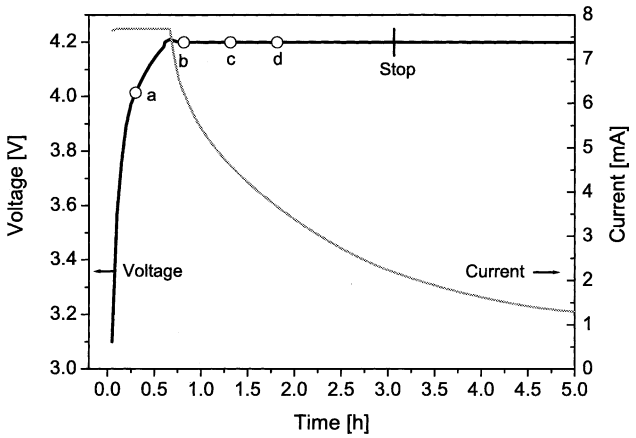

Fig. 6. Part of the first half cycle of the cell B. The NR image recording was stopped at the indicated position. The letters indicate selected images of this series shown in Fig. 7a-d.

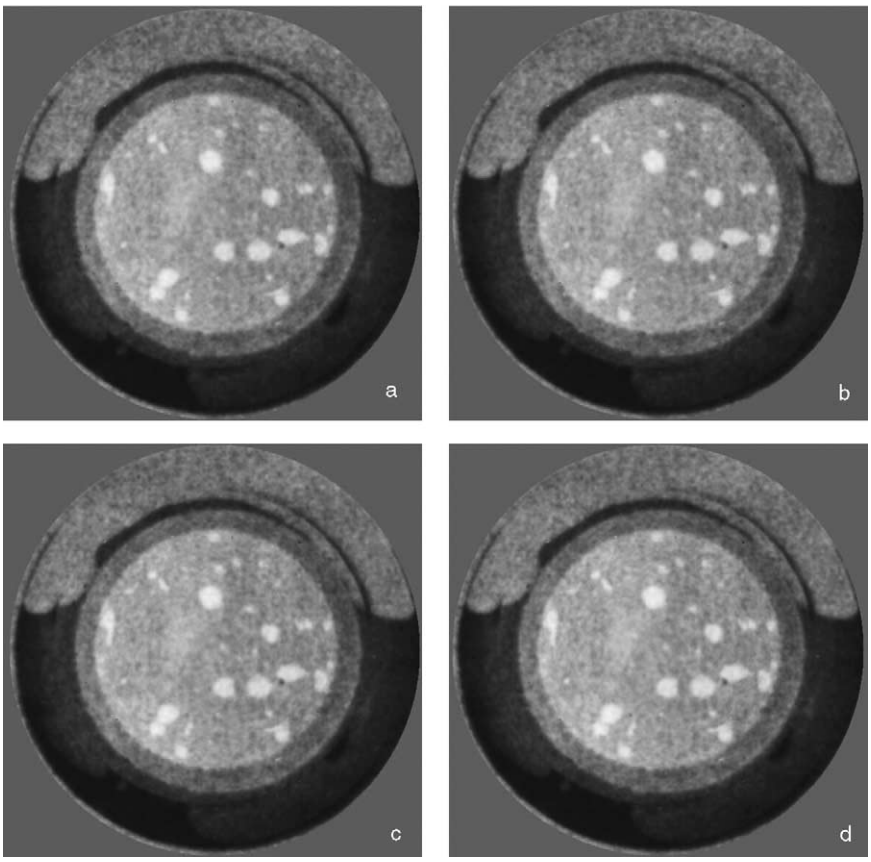

Fig. 7. (a–d) Selected normalized NR images of cell B. The correlation with the electrochemical data is indicated in Fig. 6.

very low. This earlier result can be confirmed with our NR experiments shown in Fig. 7a-d. The series of four representative normalized images does not show any difference to an unguided eye. To illustrate the occurring changes during the charge process of this cell, difference images were calculated by the ratio of the normalized reference image (image before electrochemical cycling) and the normalized image at each time. These difference images reveal a minor growth of the existing gas bubbles in the gel-type electrolyte and increase of the electrolyte level outside the electrode area. The increased electrolyte level seems to be more dominant than the growth of the gas bubbles and could particularly arise due to volume expansion of the electrodes during the charge process [5]. A more clear indication for the growth of gas bubbles in the GBL-containing electrolyte is given in Fig. 5. The calculated amount of gas trapped between the electrodes increased by ca. 3% during the first charge step.

It should be noted that, due to the limited measurement time on the neutron source, the image recording was performed only for the first 3–4 h of the first charge step. But the data behind Fig. 6 indicate that 60% of the theoretical capacity was attained in the case of the GBL-based electrolyte. It was not possible to charge faster because of the large IR drop in the test cell. However, it is known from DEMS experiments that the gas evolves mainly during the first charge step and that this process strongly correlates to the formation of the SEI on the graphite negative electrode [4,6]. The SEI formation was almost completed during the course of the experiment. Hence, our measurements are representative for the gas evolution in a practical battery.

4. Conclusions

Neutron radiography was demonstrated to be a very useful tool to investigate in situ the gas evolution and the level of electrolyte solution in gel-type lithium-ion cells during cycling. The determination of the lateral gas distribution is possible and reveals the formation of growing gas channels and bubbles. PC-containing electrolytes cause the production of large amounts of gas, which results in an unfavorable distribution of the local current density and reduction of the cell charge capacity. GBL-based gel-type electrolytes show a usable electrochemical behavior and the evolution of only very small amounts of gas. Determination of the percentage of the electrode area covered with gas bubbles offers the possibility to compare different electrolyte systems relative to their gas emission rate and could help to optimize the design of lithium-ion batteries.

Acknowledgements

We thank Mr. Gabriel Frei for the assistance, permitting easy operation at the NEUTRA beam line at PSI.

References

[1] P. Novák, J.C. Panitz, F. Joho, M. Lanz, R. Imhof, M. Coluccia, J. Power Sources 90 (1) (2000) 52.
[2] J.C. Panitz, F. Joho, P. Novák, Appl. Spectrosc. 53 (10) (1999) 1188.
[3] F. Ronci, B. Scrosati, V.R. Albertini, P. Perfetti, Electrochem. Solid State Lett. 3 (4) (2000) 174.
[4] R. Imhof, P. Novák, J. Electrochem. Soc. 145 (4) (1998) 1081.
[5] M. Lanz, P. Novák, J. Power Sources 102 (1/2) (2001) 277.
[6] R. Imhof, P. Novák, J. Electrochem. Soc. 146 (5) (1999) 1702.
[7] E. Lehmann, P. Vontobel, L. Wiezel, in: Proceedings of the Sixth World Conference on Neutron Radiography, Osaka, May 17–21, 1999, pp. 151–158, Gordon & Breache Science Publishers, 2001.
[8] J.C. Domanus (Eds.), Practical Neutron Radiography, Kluwer Academic Publishers, Dordrecht, The Netherlands, 1992.
[9] M. Lanz, E. Lehmann, R. Imhof, I. Exnar, P. Novák, J. Power Sources 101 (2) (2001) 177.
[10] A.N. Dey, B.P. Sullivan, J. Electrochem. Soc. 117 (2) (1970) 222.
[11] J.O. Besenhard, H.P. Fritz, J. Electroanal. Chem. 53 (2) (1974) 329.
[12] J.O. Besenhard, M. Winter, J. Yang, W. Biberacher, J. Power Sources 54 (2) (1995) 228.
[13] G.S. Bauer, Nucl. Instrum. Methods B 139 (1–4) (1998) 65–71.
[14] A. Chagnes, B. Carre, P. Willmann, D. Lemordant, Cycling ability of $LiBF_4$ and $LiPF_6$ in gamma-butyrolactone-ethylene carbonate based electrolytes, in: Proceedings of the 11th International Meeting on Lithium-Batteries, Monterey, 2002.